Scientific Research and Essays Vol. 6(2), pp. 305-312, 18 January, 2011
Available online at http://www.academicjournals.org/SRE
DOI: 10.5897/SRE10.704
ISSN 1992-2248 ©2011 Academic Journals

Full Length Research Paper

Effects of probe properties on ultrasonic inspection of austenitic stainless steel weldments

Memduh Kurtulmuş* and Irfan Yükler

Marmara University, Technical Education Faculty, Metal Education Department Goztepe Campus, 34722 Kadikoy, Istanbul, Turkey.

Accepted 14 December, 2010

A tee joint weldment was produced from SAE 304L austenitic stainless steel plates by the shielded metal arc process. The weld was a completely penetrated 45° single bevel groove weld. A defect free weldment was produced. The weld metal consisted of orientated and coarse austenitic grains. A hole was drilled in the base metal and the weld metal. A notch was drilled in the heat affected zone, adjacent to the weld metal boundary. Ultrasonic inspections were done with various probes and probe positions. The following results were obtained from the experiments: The extended sound path decreased the detection of the discontinuities, the defect detection character of transversal wave probes increased with the probe frequency, and the defect detection character of longitudinal wave probes decreased with the probe frequency.

Key words: Ultrasonic testing, austenitic stainless steel welding, NDT and NDE of stainless steels, ultrasonic inspection of austenitic steel welds.

INTRODUCTION

Austenitic stainless steels are an important group of materials which are generally used for applications where resistance to corrosion or high strength and creep resistance at elevated temperatures are required. These steels are used extensively in nuclear plants, pressure vessels and chemical reactors. Austenitic stainless steel components are joined together by different welding processes (www.echoplus.ru/eng/arch/bars 2002.pdf). In these constructions, safety considerations and economic operations are vital factors in the design. When sections of austenitic stainless steels are joined by welding, crack-like defects may form. If the cracks are large enough, they will propagate under the stress of operation and failure of the joint may result in physical and economic damage due to lack of plant availability during repairs. Thus it is not only important to be able to detect the defects, but also to size them in order to decide whether or not the weld is fit to enter repair or remain in service (Connolly et al., 2008). Therefore, detection of various defects in the weld zone and quantitative evaluation are of great importance in terms of the structure's integrity and stability.

The weldments are inspected by non-destructive test (NDT) methods. The penetrant test and the magnetic particle test methods have a number of problems, such as the limitations of defect detection of the surface and subsurface. The radiographic test method and the ultrasonic test method reveals the internal defects of the weldments. The ultrasonic test method has some advantages to the radiographic test method. These advantages include safety considerations, quality factors, time savings and cost savings (Kruzic, 2004; Kurtulmus et al., 2007). The ultrasonic test method became the major NDT method in nuclear plants because of the advantages explained above (Kemnitz, 1997; Moysan et al., 2003). The atoms of solid austenitic stainless steel

*Corresponding author. E-mail: memduhk@marmara.edu.tr. Tel: +90 216 336 57 70/362. Fax: +90 216 337 89 87.

Table 1. The chemical composition of the test plate.

Elements	Cr	Ni	C	Mn	Mo	Cu	Si	V	Fe
Weight percent %	18.33	8.11	0.03	1.22	0.77	0.63	0.40	0.11	Remainder

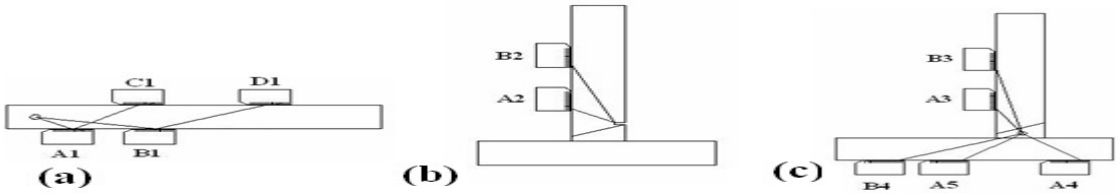

Figure 1. The ultrasonic testing of (a) The base metal hole, (b) The HAZ notch and (c) The weld metal hole. The letters indicate the probe positions and the lines show the sound wave paths.

have a face-centered cubic structure at all temperatures. Therefore, the macrocrystalline structure of an austenitic weld is established during solidification. Long columnar grains grow along the directions of maximum heat loss during solidification and cooling. The weld metal microstructure contains orientated coarse grains which have dentritic character (Ekinci, 1994). The microstructure is much more complex in multipass welds.

Due to the physical properties of the weld grains, many ultrasonic inspection problems arise (Kemnitz et al., 1997; Moysan et al, 2003; Ekinci, 1994; Qilin and Maodi, 2000; Erhard et al., 2000; Krautkramer et al., 1990): Large and orientated anisotropic grains may cause severe attenuation by scattering, changing the sound velocity and beam skewing. In addition, refraction and reflection of sound beams may occur at the grain boundaries, from the weld root, counter bore geometries and weld fusion lines (Anderson et al., 2003). The attenuation of the wave varies with the beam angle of the weld metal grains (Moysan et al., 2009). The sound velocity also changes with the orientation of the grains (Chassignole et al., 2005). Therefore, very low signal to noise ratios are obtained in ultrasonic testing of austenitic welds (Kurtulmus et al., 2006).

The ultrasonic flaw responses are often obscured by scattered energy from the material structure, which disable the detection of the flaw. Some attempts have been made to resolve the inspection problems, namely longitudinal wave probes have been produced for austenitic welds (Handbook on Ultrasonic Examination of Austenitic Welds, 1985). The transversal sound waves are strongly refracted at the interfaces such as grain boundaries and dendrite arms. Only few arrays propagate back to the probe after being scattered. This causes a low signal to noise ratio. The longitudinal wave does not scatter at the interfaces (Kohler et al., 2006). The longitudinal wave probes give higher signal to noise ratios than the transversal wave probes. Some ultrasonic testing methods have been improved to obtain higher signal to noise ratios in testing of austenitic welds Just and Csapo, 2006; Ploix et al., 2006; Leger and Deschamps, 2009; www.V.Grebenikov, 2002; Krautkramer Catalogue, 2004; Kono et al., 2008; Kawanami et al., 2001; Cochran, 2006; Chardome and Verhagen, 2008; Toullelan et al., 2008; Moles and Cancre, 2002). The phased array ultrasonics is the most important improvement.

This method was mainly developed for nondestructive evaluation of austenitic stainless steel weldments of power plants. The effects of wave type and probe frequency on ultrasonic test results in mild steel weldments are well known (Krautkramer et al., 1990). The aim of this work is to understand the effects of probe properties on ultrasonic testing of austenitic weldment.

MATERIALS AND METHODS

A SAE 304L austenitic stainless steel plate of 20 mm thickness was used in the experiments. The chemical composition of the plate is shown in Table 1. Two test parts were cut from the plate by the plasma cutting process. The dimensions of the pieces were 250 x 150 mm. The longitudinal dimension of the part was parallel to the rolling direction of the plate. A 45° single bevel groove angle was obtained by milling on the longitudinal side of a test piece. It was welded to the other piece by the shielded metal arc process to obtain a tee joint. ASP 308L electrodes were used in the welding operation. No preheating was used in the welding process. The slag was removed by wire brushes after each pass and the weldment was tested by the liquid penetrant method. After finishing the passes, the weldment was radiographically tested. A defect-free weldment was obtained.

The weldment was grounded using 80 to 150 to 240 grinding papers. Then the weld region was lightly etched with HCl_3 and NHO_3 solution to reveal the macrostructure. The boundary between the weld metal and the heat affected zone (HAZ) was exposed. A notch was drilled in HAZ adjacent to the weld metal solidification line. The notch was 1 mm thick, 2 mm tall and 20 mm deep. Then a hole was drilled in the middle of the weld metal. The diameter of the hole was 1 mm and it was 20 mm deep. A similar hole was drilled in the base metal. The tee joint and the drilled discontinuties are schematically shown in Figure 1. The artificial discontinuities were

Table 2. The properties of the test probes (21).

Probe wave mode	T	T	T	T	L	L	L	L
Probe Angle	45°	70°	45°	70°	45°	70°	45°	70°
Probe frequency, MHZ	4	4	2	2	4	4	1.8	1.8
Effective test range, mm	3 to 4600	3 to 4200	5 to 3300	4 to 2400	3 to 40	4 to 35	21 to 150	15 to 100

T: Transversal, L: Longitudinal.

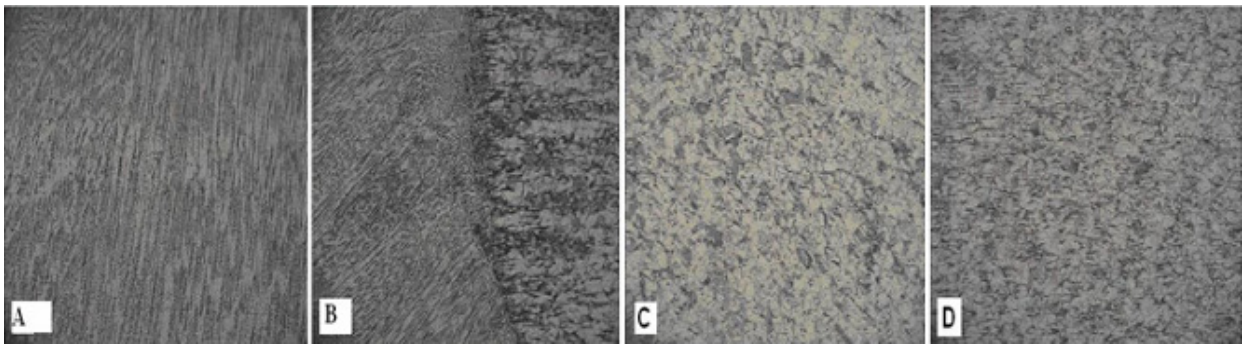

Figure 2. The microstructure of (A) The weld metal, (B) The transition zone between the weld metal and the HAZ., (C) The HAZ and (D) The base metal.

inspected by the ultrasonic method using a KRAUTKRAMER USM 25S detector which is a digital/analog pulse – echo flaw detector. Prior to commencement of the inspection, the specimen surface was light greased. The probes used in the experiment and their properties are shown in Table 2. The artificial defect locations, the probe positions and the sound paths from the probe surfaces to the defects are shown in Figure 1. In these Figures A1, A2, A3, A4, A5 and C1 letters express the positions of 45° angled probes and B1, B2, B3, B4 and D1 show the positions of 70° probes. In each test the sound path length was shown directly on the secreen of the detector.

In this study, the reference display was chosen as 40%. The signal to noise (S/N) ratio was calculated for each test. The S/N ratio is the main criteria in the definition of the defect detection character of a probe (Kemnitz et al., 1997). The defect detection character of a probe increases with the S/N ratio. Several repeated tests which were conducted under the same conditions showed that the S/N ratio accuracy varied in a ±2 dB range in the experiments. Following the ultrasonic inspection process, a metallographic specimen was cut out from the weldment from the opposite side of the defects. The surface of the weldment was grounded and polished. It was etched with 75% HCl3 and 25% NHO3 solution to reveal the microstructure of the different zones. The specimen was inspected by a metal microscobe. Then photographs were taken at various points of the weldment.

RESULTS

The microstructure of the weld metal, the heat affected zone and the base metal of the weldment are shown in Figure 2. The weld metal which is shown in Figure 2A has oriented dendritic coarse grains. This is the usual microstructure of an austenitic stainless steel weld (Moysan et al., 2003; www.V.Grebenikov, 2002). The microstructure of the transition zone between the weld metal and the heat affected zone is shown in Figure 2B. The HAZ and the base metal microstructure are shown in Figures 2C and 2D. The grains of the HAZ and the base metal are fairly identical. Even the grains of the HAZ adjacent to the weld metal (Figure 2B) are similar to the base metal grains. Neither a distinct grain growth nor grain orientation is observed in the heat affected zone.

The ultrasonic test results of the base metal hole are shown in Table 3. In these tests, very high signal to noise (S/N) ratios were obtained. The test results illustrate that S/N ratio decreases with the increase in sound path length. Test results of Table 3 shows that the flaw detectability of the transversal wave probes increases with the increase in probe frequency, and the flaw detectability of the transversal wave probes decreases with the increase in probe frequency. Test results have shown that the transversal wave probes are more suitable than the longitudinal wave probes for ultrasonic inspection of base metal discontinuities of austenitic stainless steels. The ultrasonic inspection test results of the heat affected zone notch are shown in Table 4. These tests also show that transversal probes are superior than the longitudinal ones, because they give high S/N ratios. In these tests S/N ratios decreased with the increase of the sound path. Test results also show that 4MHZ transversal wave probes are better in flaw detectability than the 2 MHz probes. The opposite trend is valid for the longitudinal wave probes.

The ultrasonic inspection test results of the weld metal hole are shown in Table 5. There is a sharp decrease in

Table 3. The ultrasonic inspection results of the base metal hole.

4 MHz. transversal wave probes			2 MHz. transversal wave probes		
Probe position	**Sound path, mm**	**S/N ratio, dB**	**Probe position**	**Sound path, mm**	**S/N ratio, dB**
A1	12.91	31.0	A1	15.17	27.0
B1	28.44	29.5	B1	29.02	24.5
C1	38.93	29.0	C1	43.89	22.5
D1	84.67	25.0	D1	86.10	17.0
4 MHz. longitudinal wave probes			**1.8 MHz. longitudinal wave probes**		
Probe Position	**Sound Path, mm**	**S/N Ratio, dB**	**Probe Position**	**Sound Path, mm**	**S/N Ratio, dB**
A1	14.70	15.0	A1	15.10	21.0
B1	30.31	14.5	B1	30.38	20.5

Table 4. The ultrasonic inspection results of the HAZ notch.

4 MHz. transversal wave probes			2 MHz. transversal wave probes		
Probe position	**Sound path, mm**	**S/N ratio, dB**	**Probe position**	**Sound path, mm**	**S/N ratio, dB**
A2	29.79	28.0	A2	29.45	23.5
B2	58.61	25.5	B2	59.58	20.5
4 MHz. longitudinal wave probes			**1.8 MHz. longitudinal wave probes**		
Probe position	**Sound path, mm**	**S/N ratio, dB**	**Probe position**	**Sound path, mm**	**S/N ratio, dB**
A2	28.38	14.5	A2	27.57	20.5
B2	58.06	14.0	B2	56.86	19.0

S/N ratio results shown in Table 5 compared to the results in Tables 3 and 4. Flaw dedectabilty of transversal wave probes sharply decreased in these tests. The extension of sound paths caused further decrease in S/N ratios. 4MHz longitudinal wave probe S/N ratio results decreased with the sound path length, but 1.8 MHz longitudinal wave probe S/N ratios were not effected with the path length. 1.8 MHz longitudinal wave probes gave the best results in weld metal hole tests.

DISCUSSION

In the base metal hole tests, the ultrasonic sound wave progressed only in the base metal. As the ultrasonic sound wave progresses in the base metal, attenuation occurs in the scattering of the grains (Krautkramer, et al., 1990). The scattering increases with the length of the sound path. Table 3 shows that in 4 MHz transversal wave probes, the S/N ratio was 31.0 dB for a 12.91 mm sound path. The S/N ratio decreased to 29.5 dB for a 28.44 mm sound path. The decrease in the S/N ratio is due to the extended sound path. The relation between the sound path and the S/N ratio for the ultrasonic tests of the base metal hole with the transversal wave probes are shown in Figure 3. The S/N ratio linearly decreases with the sound path length. The frequency of the probes is found to have no effect on this decrease.

The transversal and longitudinal wave probes of various frequencies display the same charasteristics (Table 3). The flaw detectability of the transversal wave probes increases with the increase in probe frequency. The 2 MHz probe gave a 24.5 dB S/N ratio for a 29.02 mm sound path. The 4 MHz probe gave a 28.5 dB S/N ratio for a 28.44 mm sound path. Although the sound path lengths of these two tests are roughly equal, there is a 4.0 dB S/N ratio difference between them. The difference between the two results depends mainly on the frequency of the probes. The probe of higher frequency gave a higher S/N ratio. The A1 and D1 probe position tests of the transversal probes gave similar results. The longitudinal wave probe results, which are shown in Table 3, are contrary to the transversal ones. In longitudinal wave probes, the flaw detectability decreases with the increase in the probe frequency. For A1 probe position tests, a 40% higher S/N ratio was obtained in the 1.8 MHz probe than the 4.0 MHz probe. The B1 probe position ultrasonic tests of the longitudinal probes gave similar results.

The base metal hole ultrasonic inspection tests reveal that transversal wave probes are superior to the longitudinal wave probes. The test results of 4 MHz

Table 5. The ultrasonic inspection results of the weld metal hole.

4 MHz. transversal wave probes			2 MHz. transversal wave probes		
Probe position	**Sound path, mm**	**S/N ratio, dB**	**Probe position**	**Sound path, mm**	**S/N ratio, dB**
A3	14.71	20.5	A3	15.23	18.0
B3	29.30	18.0	B3	32.08	14.5
A4	35.36	17.0	A4	37.04	12.5
A5	35.51	14.5	A5	37.18	10.0
B4	73.10	7.0	B4	76.92	5.0
4 MHz. longitudinal wave probes			**1.8 MHz. longitudinal wave probes**		
Probe position	**Sound path, mm**	**S/N ratio, dB**	**Probe position**	**Sound path, mm**	**S/N ratio, dB**
A3	13.82	13.0	A3	15.98	15.5
B3	30.14	12.0	B3	29.20	16.0
A4	35.28	10.5	A4	37.81	16.5
A5	35.53	12.0	A5	38.02	19.0
B4	70.26	4.0	B4	74.78	15.0

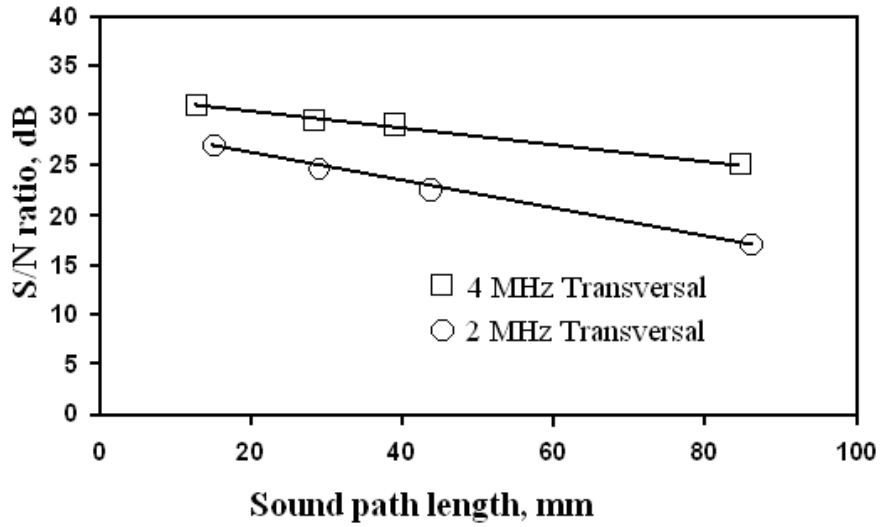

Figure 3. The ultrasonic test results of the base metal hole with transversal wave probes.

transversal wave probes gave a 50% high S/N ratio than the 1.8 MHz longitudinal wave probe which is better than the 4 MHz longitudinal wave probe.These results have shown that the transversal wave probes are more suitable for ultrasonic inspection of base metal discontinuities of austenitic stainless steels. The effective test range is also very high in transversal wave probes (Table 2). The 4 MHz transversal wave probe is very appropriate for ultrasonic inspection of unwelded wrought stainless steels. In heat affected zone notch tests, the ultrasonic sound wave progressed both in the base metal and in the HAZ. Figures 2E and 2D show that the microstructure of the HAZ was nearly identical to the base metal's microstructure.

The diagrams in Figure 4 reflects the base metal hole and HAZ notch test results to compare the sound wave scattering effects of the base metal and the HAZ microstructure. In Figure 4, the effect of the sound path length on the S/N ratio of the ultrasonic tests is revealed. Transversal wave probes displayed a linear S/N ratio decrease with the sound path length. The decrease in the longitudinal wave probes is very small. All types of probes showed a linear decrease. The HAZ microstructure did not alter the trends of the base metal microstructure attenuation effect. Figure 4 shows that the base metal and the HAZ had similar sound wave attenuation effects. Thus, we can assume that in the HAZ notch inspection tests, the sound wave progressed only

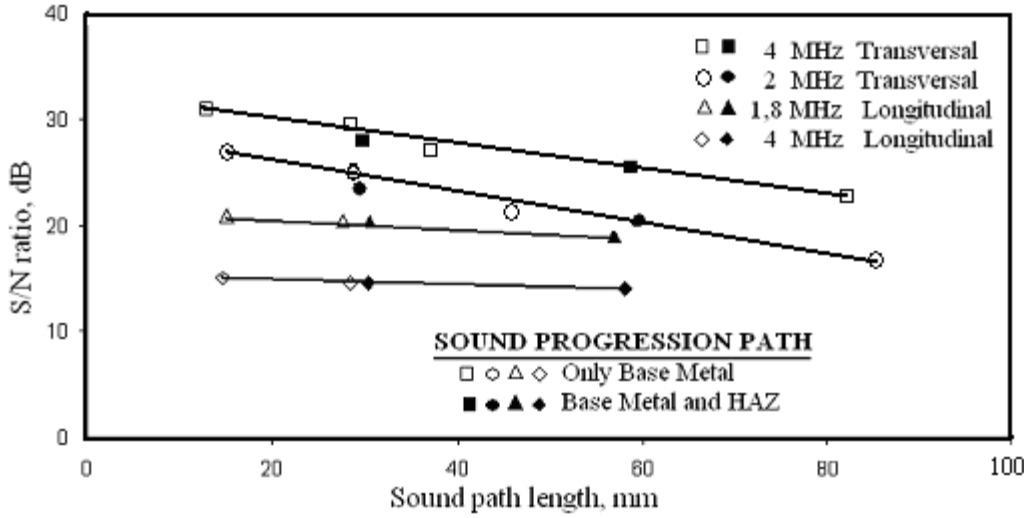

Figure 4. The ultrasonic test results of the base metal hole and the HAZ notch.

in the base metal. In the weld metal hole tests, the ultrasonic sound wave progressed in the base metal, the heat affected zone and the weld metal. As long as the HAZ and the base metal have the same sound scattering characteristics, it can be assumed that the sound wave progressed only in the base metal and the weld metal. The computed S/N ratios shown in Table 5 are lower than the results in the Tables 3 and 4. This difference occurred because of the weld metal characteristics (Kurtulmus et al., 2006). The weld metal causes these differences.

The comparison of the S/N ratio results of 4 MHz transversal wave probes clearly shows the effect of the weld metal microstructure on the ultrasonic inspection tests. The sound path lengths of the 4 MHz transversal probes of probe position B1 (Table 3), A2 (Table 4) and B3 (Table 5) are 28.44, 29.79 and 29.30 mm respectively. The sound path lengths are very close in the mentioned tests. The S/N ratios of these tests are 29.5 dB (Table 3), 28.0 dB (Table 4) and 18.0 dB (Table 5). The S/N ratios of the base metal hole and the HAZ notch tests are close. The S/N ratio of the weld metal hole is 10.0 dB less than the other tests. The 10.0 dB difference is related to the weld metal microstructure because the sound wave was severely attenuated as it progressed in the weld metal (Ekinci, 1994; Kurtulmus et al., 2006). This attenuation increases with the increase in the sound path (Anderson, et al., 2003; Ploix et al., 2006) and the grains orientation of the microstructure (Leger and Deschamps, 2009). The weld metal hole was tested with 5 different probe positions. The sound path of these probes in the weld metal are schemetically shown in Figure 5. The sound path lengths of the A3, A4, A5 and B3 probe positions are roughly equal (AH=BH=CH=DH). The sound path length (EH) of the probe position B4 in the weld metal was nearly double that of the others. The enlarged probe angle of the B4 probe caused this difference. The transversal wave probes gave very small S/N ratios for the B4 probe position ultrasonic tests of the weld metal hole (Table 5). The extended weld metal sound path length caused high attenuations in the sound. The S/N ratio for the 4 MHz transversal wave probe was only 7.0 dB for the B4 probe position.

In Figure 3, a 26.0 dB S/N ratio is estimated for a 73.10 mm sound path in the ultrasonic inspection of the 4 MHz transversal probe. This result can be obtained in the ultrasonic test of an unwelded metal. There is a 19.0 dB difference between the calculation and the actual test. For this probe, only a 10.0 dB difference was found in the A3 and B3 probe positions (Table 5) as compared to the A1 and B1 probe positions (Table 3). The extra 9.0 dB difference originated from the extended weld metal sound path of the B4 probe position which is shown in Figure 5. The 1.8 MHz longitudinal wave probe gave the optimum S/N results for the weld metal hole tests. The S/N ratios were almost identical in all the tests. The sound path elongation and the weld metal microstructure had a slight effect on this probe. Although the longitudinal wave probes are manufactured for the ultrasonic tests of austenitic stainless steel welds (Handbook on Ultrasonic Examination of Austenitic Welds, 1985), 4 MHz probes gave poor results (Table 5). This indicates that low frequency longitudinal probes are superior in the dedection of the weld metal discontinuties of austenitic stainless steels.

The effective test range of the longitudinal wave probes is very small compared to the transversal wave probes (Table 2). This disadvantage causes unexpected low test results, as demonstrated in the results of the B4 probe position of the 4MHz longitudinal wave probe (Table 5). A 4.0 dB S/N ratio was obtained in this Vtest,

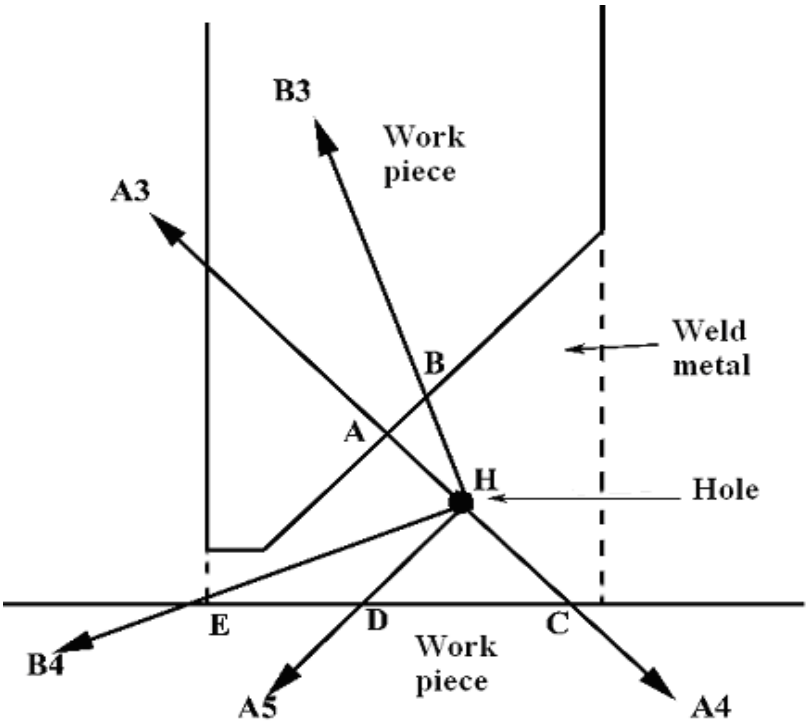

Figure 5. The probe positions and sound paths in the ultrasonic test of the weld metal hole.

because the sound path length was beyond the upper test limit of the probe.

Conclusions

The following results were obtained from the experiments:

1. The extended sound path decreased the detection of the discontinuities.
2. The defect detection characteristic of transversal wave probes increased with the probe frequency.
3. The defect detection characteristic of longitudinal wave probes decreased with the probe frequency.
4. The transversal wave probes are useful for inspection of unwelded wrought austenitic stainless steels.
5. The longitudinal wave probes are superior in ultrasonic inspection tests of austenitic stainless steel weldment.

REFERENCES

Anderson MT, Cumblidge SE, Steven R (2003). Applying Ultrasonic Phased Array Technology to Examine Austenitic Coarse Grained Structures for Light Water Reactor Piping, Paper Presented at 3rd EPRI Phased Array Inspection Seminar, Seattle.

Chardome V, Verhagen B (2008). Development of a Procedure for the Ultrasonic Examination of 9% Nickel LNG Storage Tank Welds Using Phased Array Technol. Insight., 50: 490-492.

Chassignole B, Doudet L, Dupond O, Fouque T, Richard B (2005). New Developments for the Ultrasonic Inspection of Austenitic Stainless Steel Welds, Paper Presented at European Nuclear Conference, Versailles, France, pp. 11-14.

Cochran S (2006). Fundamentals of Ultrasonic Phased Arrays, Insight, 48: 212-217.

Connolly GD, Lowe MJS, Rokhlin SI, Temple JAG (2008). Modelling the Propagation of Elastic Waves in Generally Anisotropic Materials and Austenitic Steel Welds, Rev. Quant. Nondestruct. Eval., 27: 1026-1033.

Ekinci S (1994). The Problems of Ultrasonic Testing of Austenitic Welds and Their Solutions, Metallurgy J., 12: 7-13.

Erhard A, Lucht B, Schulz E, Montag HJ, Wüstenberg H, Beine U (2000). Characterization of Defects in Austenitic Pipe Gird Welds, NDT-net, 5(10): 10.

Just T, Csapo G (2006). Qualification of NDT Techniques for In-service Inspections in Nuclear Power Plants in Accordance with ENIQ, Paper Presented at 5th International Conference on NDE in Relation to Structural Integrity for Nuclear and Pressurized Components, San Diego.

Handbook on Ultrasonic Examination of Austenitic Welds (1985). IIS-IIW-836-85-1985.

Kawanami S, Kurokawa M, Taniguchi M, Tada Y (2001). Development of Phased Array Ultrasonic Testing Probe, Mitsubishi Heavy Ind. Tech. Rev., 38: 121-125.

Kemnitz P, Richter U, Klübe H (1997). Measurements of the Acoustic Field on Austenitic Welds, Nuclear Eng. Design., 174: 259-272.

Kohler B, Müller W, Spies M, Schmitz V, Zimmer A, Langenberg KJ, Mletzko U (2006). Ultrasonic Testing of Thick Walled Austenitic Welds, Rev. Quant. Nondestruct. Eval., 25: 57-64.

Kono N, Baba A (2008). Development of Phased Array Probes for Austenitic Weld Inspections Using Multi-Gaussian Beam Modeling, Rev. Quant. Nondestruct. Eval., 27: 747-753.

Krautkramer Catalogue (2004). Probes Handy Precision Tools for

Ultrasonic Testing.
Krautkramer H, Krautkramer J (1990). Ultrasonic Testing of Materials, 4th Edition, Springer Verlag, Berlin, p. 187.
Kruzic R (2004). LNG Storage Tanks: Advancements in Weld Inspections, Hydrocarbon Processing, 7: 53-55.
Kurtulmus M, Buyukyildirim G, Yukler AI (2006). Optimum Ultrasonic Inspection Conditions of Butt Welded SAE 304L Austenitic Stainless Steel, Paper Presented at 1st South East European Welding Congress, Timisiora.
Kurtulmus M, Fidaner O, Yukler AI (2007). Testing of Repair Welded Boiler Pipes of a Thermal Power Station, Paper Presented at ICCI 2007 13th International Energy Conference, Istanbul.
Leger A, Deschamps M (2009). Ultrasonic Wave Propagation in Non Homogeneous Medial, Springer Verlag, Berlin, p.17.
Moles M, Cancre F (2002). Element Parameters for Ultrasonic Phased Arrays, Rev. Quant. Nondestruct. Eval., 21: 855-860.
Moysan J, Gueudré C, Ploix MA, Corneloup G, Guy PH, Guerjouma RE, Chassignole B (2009). Advances in Ultrasonic Testing of Austenitic Stainless Steel Welds. Towards a 3D Description of the Material Including Attenuation and Optimisation by Inversion, Ultrasonic Wave Propagation in Non Homogeneous Media, A.Leger and M. Deschamps Editors, Springer Verlag, New York, pp. 15-24.
Moysan J, Apfel A, Comeloup G, Chassignole B (2003). Modelling the Grain Orientation of Austenitic Stainless Steel Multipass Welds to Improve Ultrasonic Assessment of Structural Integrity, Int. J. Pressure Vessels Piping., 80: 77-85.
Ploix MA, Guy P, Guerjouma RE, Moysan J, Chassignole B (2006). Attenuation Assesment for NDT of Austenitic Stainless Steel Welds, Paper Presented at 9th European Conference on NDT, Berlin.
Qilin Q, Maodi Z (2000). Technique for Austenitic Stainless Steel Weld, Paper Presented at 15th World Non Destructive Conference, Rome.
Toullelan G, Casula O, Abittan E, Dumas P (2008). Application of a 3D Smart Flexible Phased-Array to Piping Inspection, Rev. Quant. Nondestruct. Eval., 27: 794-800.
www.V.Grebenikov (2002). Comparative Analysis of the Ways to Increase Signal to Noise Ratio at NDT Inspection of Austenitic Welds.
www.echoplus.ru/eng/arch/bars pdf.